

Silicon nanowires for advanced sensing: Electrical and electromechanical characteristics and functionalisation technology

H. Mizuta*, F. A. Hassani, M. A. Ghiass, Y. Tsuchiya

*University of Southampton, UK (*also JAIST, Japan)*

S. Armini, T. Delande, J. Loyo Prado, V. Cherman

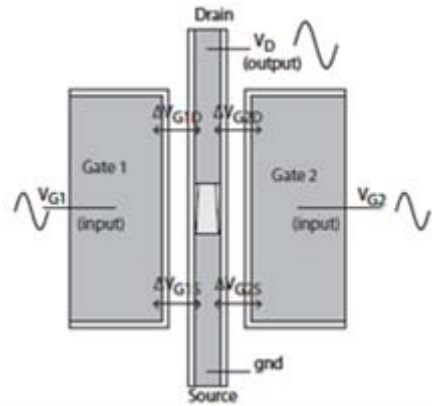
IMEC-BE, Belgium

C. Dupré, E. Ollier

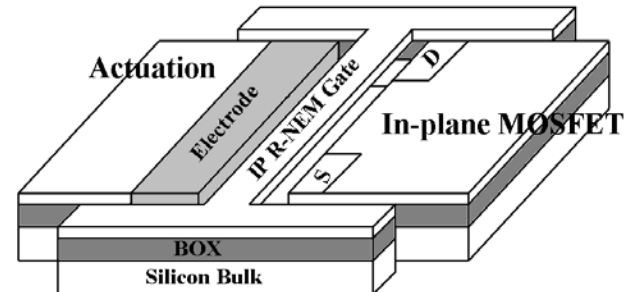
CEA-LETI, MINATEC, France



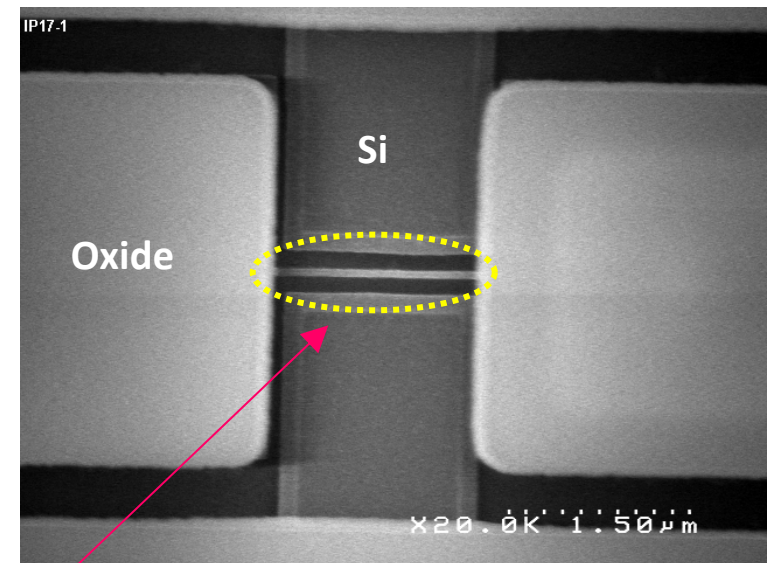
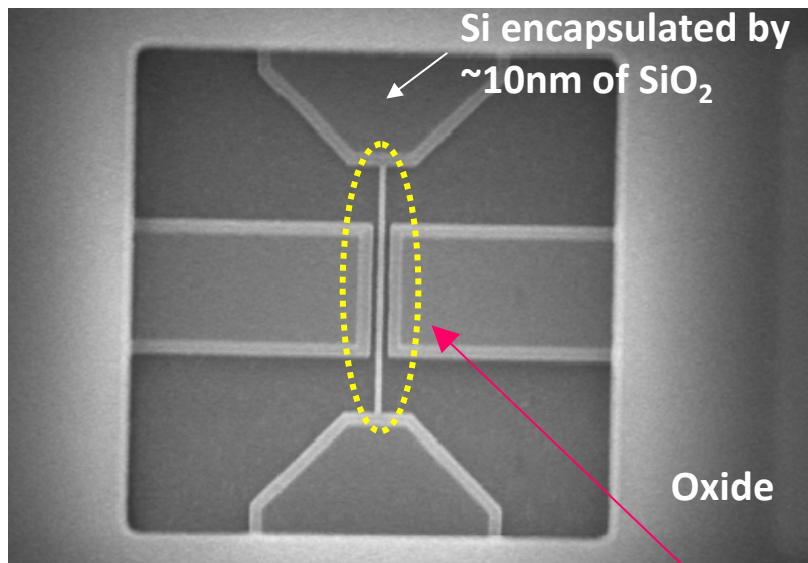
NEMSIC sensor devices



Vibrating Body FET
Vibrating Junctionless FET



In-plane Resonant Suspended Gate FET

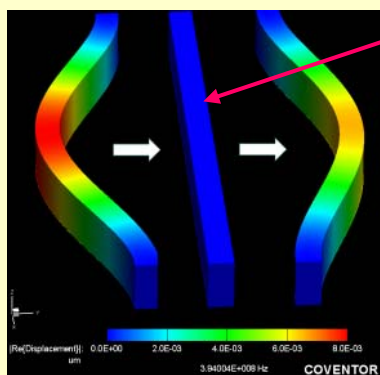


A suspended SiNW as a sensor head

NEMSIC detection principle

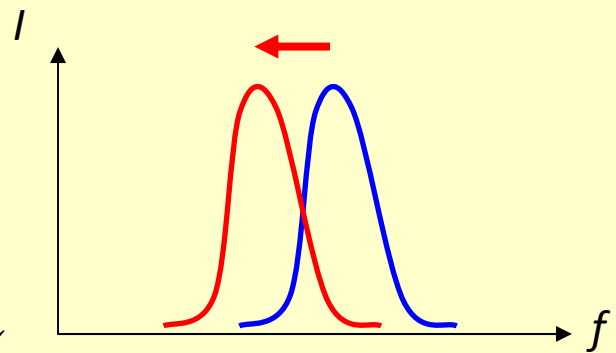
Resonance-based sensing – Mass detection

Vibrating suspended SiNW



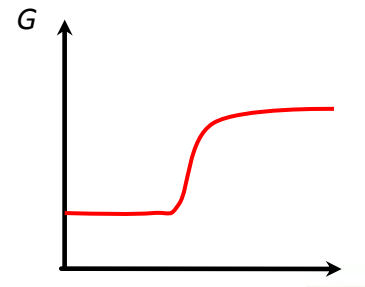
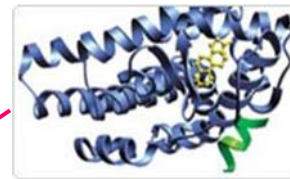
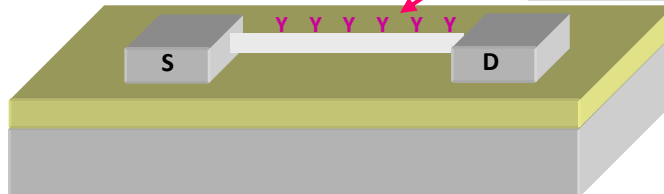
$$f_r = \frac{1}{2\pi} \sqrt{\frac{k_b}{m_b}}$$

Mass ↑ , Frequency ↓



cf. conventional principle:

Conduction-based sensing – Charge detection



Outline

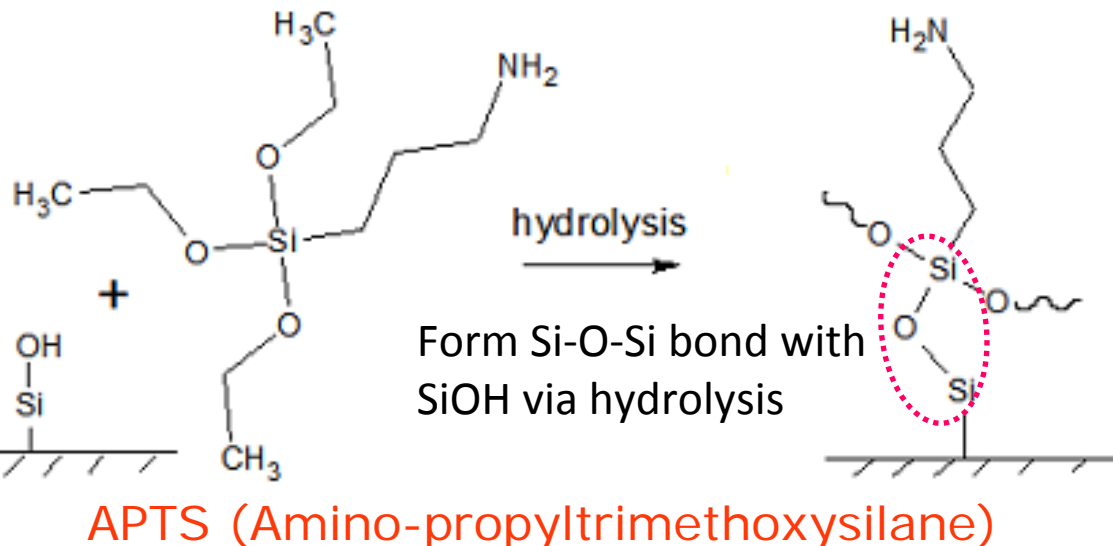
- **Development of selective surface functionalization techniques for SiNWs**
- **SiNW electrical characteristics and the impact of suspension and surface functionalization**
- **Design and fabrication of in-plane resonant suspended gate FETs (IP-RSGFETs)**
- **Summary**

Outline

- **Development of selective surface functionalization techniques for SiNWs**
- **SiNW electrical characteristics and the impact of suspension and surface functionalization**
- **Design and fabrication of in-plane resonant suspended gate FETs (IP-RSGFETs)**
- **Summary**

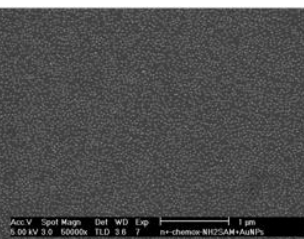
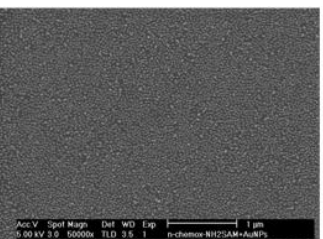
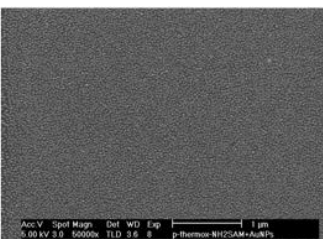
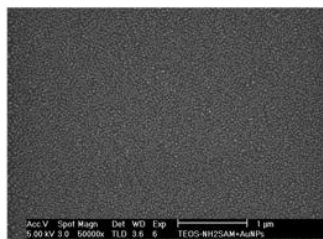
Bio-functionalization using NH₂-SAM on SiO₂

NH₂-SAM deposition on SiO₂

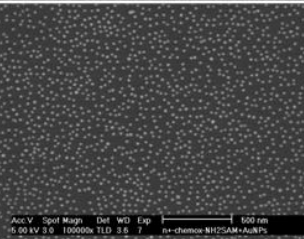
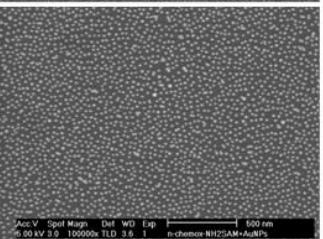
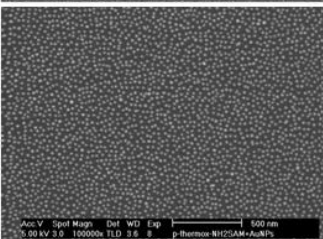
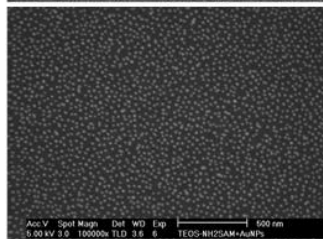


Sample	C.A (degrees)
Cleaned SiO ₂	< 10
NH ₂ -SAM 15min	52.1 (reported as monolayer CA)
30min	54.9
45min	58.3
1h	60.1

BEFORE



AFTER



TEOS oxide

p-type thermally
grown oxide

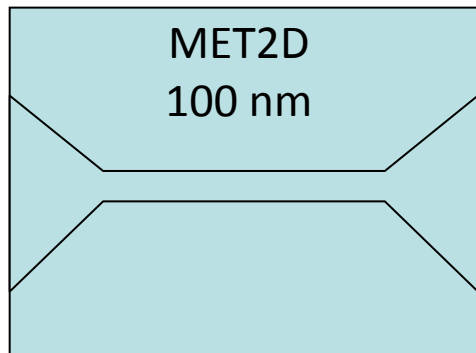
n-type native
oxide

n-doped
chemical oxide

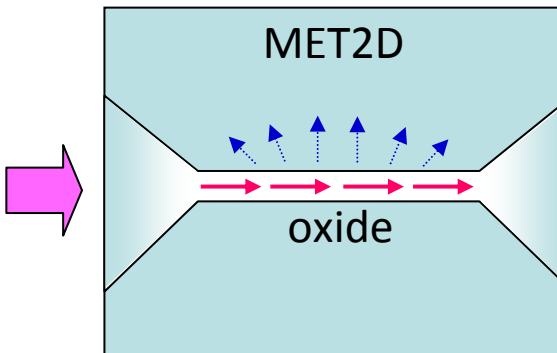
Works for all
different types
of SiO₂

Selective functionalization of SiNW surface

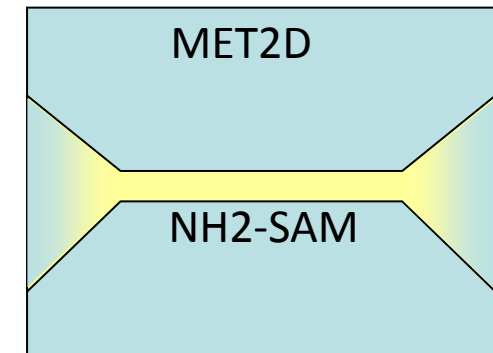
① Joule heating method



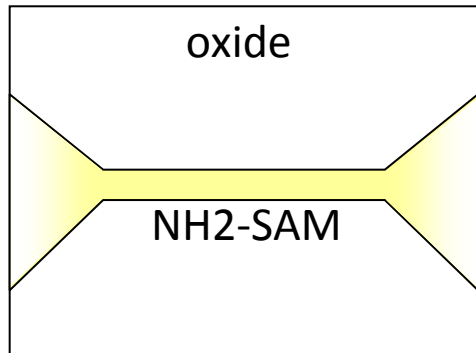
Resist spincoating



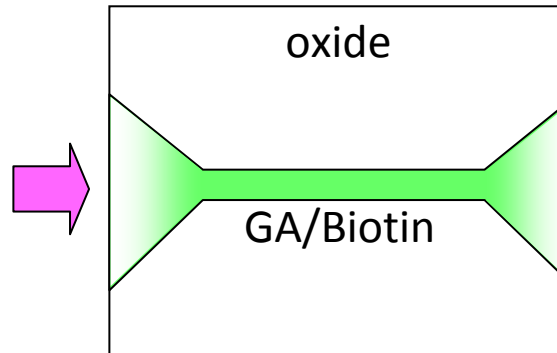
Ablation via Joule heating



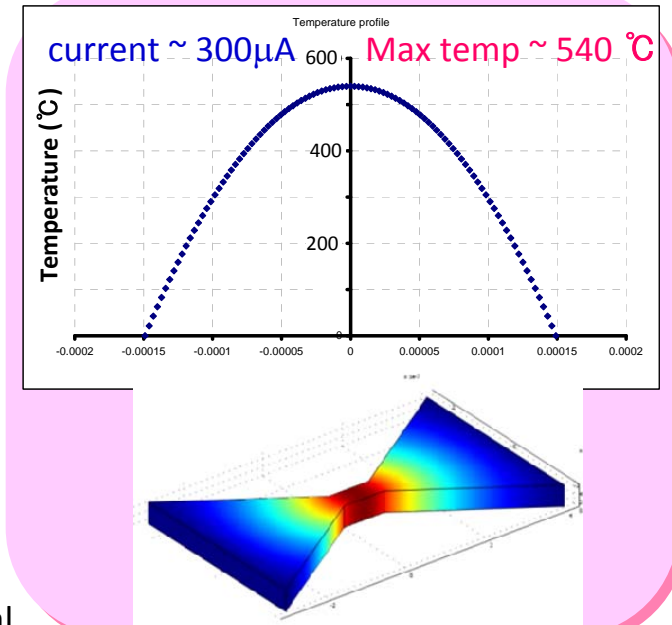
SAM coating



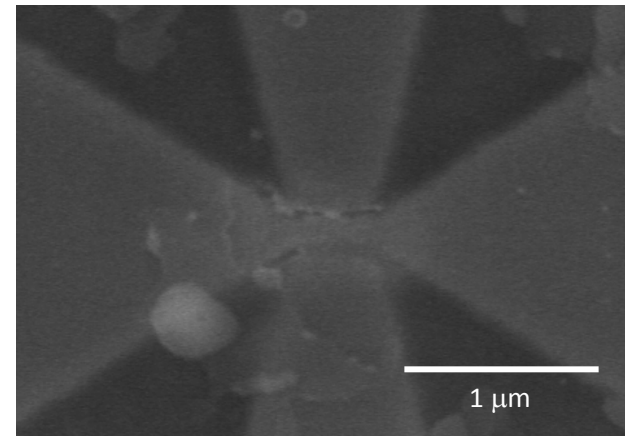
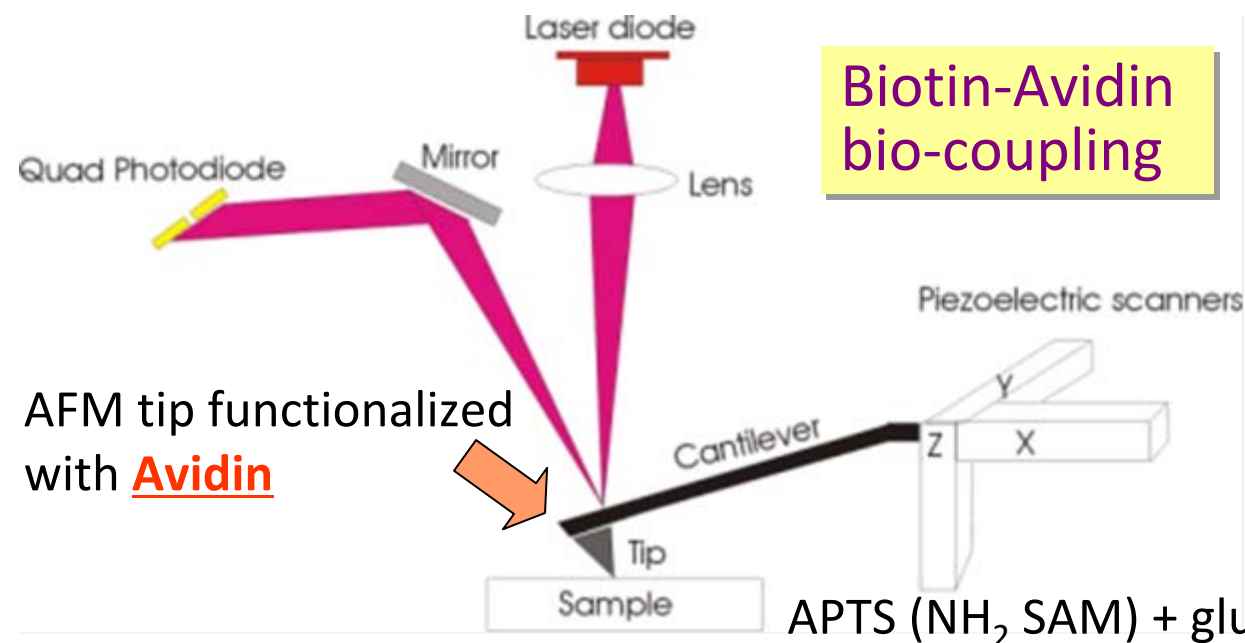
Resist removal



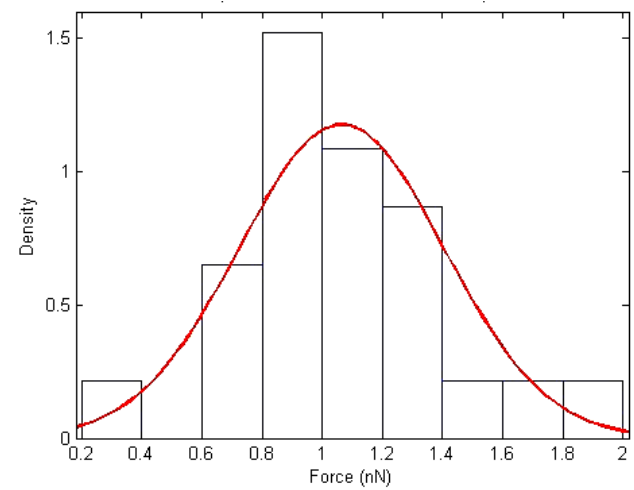
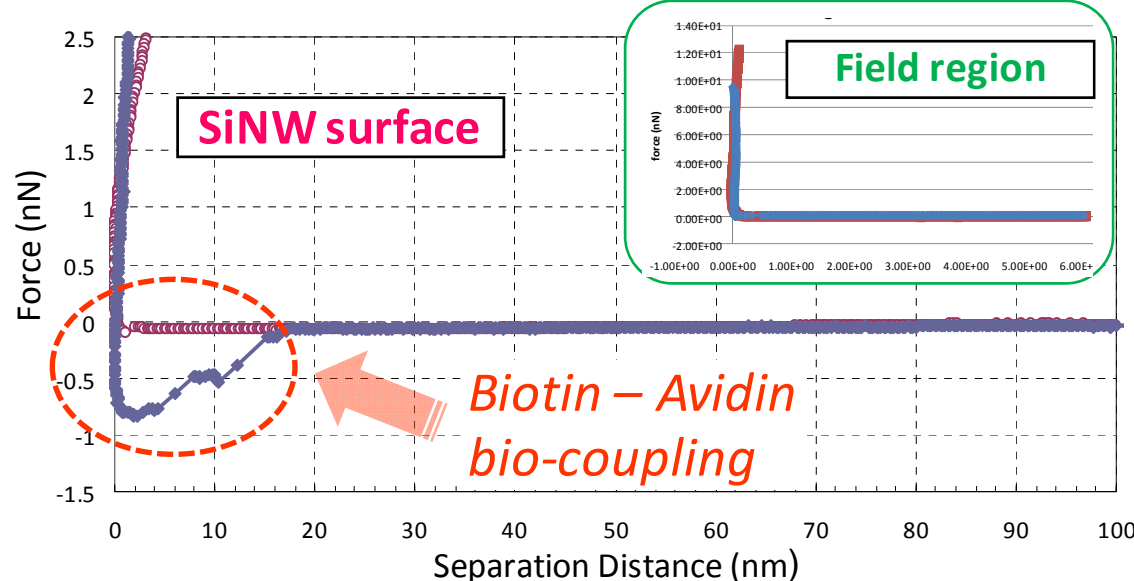
Biofunctionalization



AFM-based testing of selective functionalization

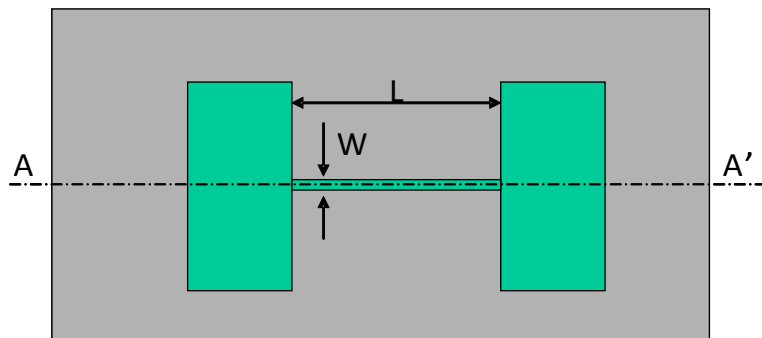


APTS (NH_2 SAM) + glutaraldehyde (GA) + Biotin

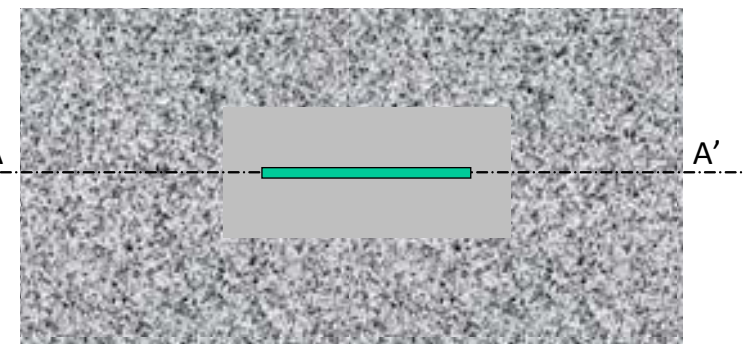
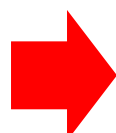


Selective functionalization of SiNW surface

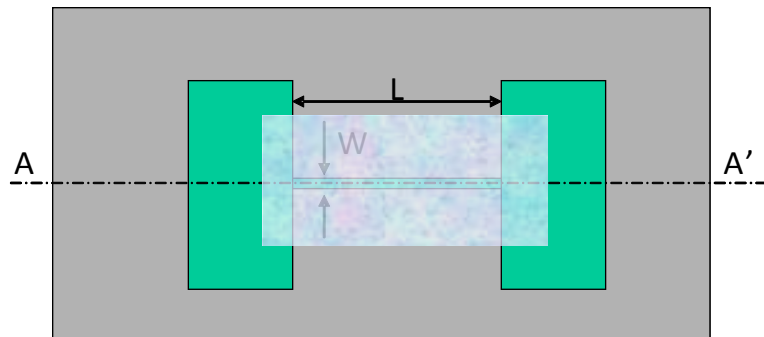
② E-beam lithography approach



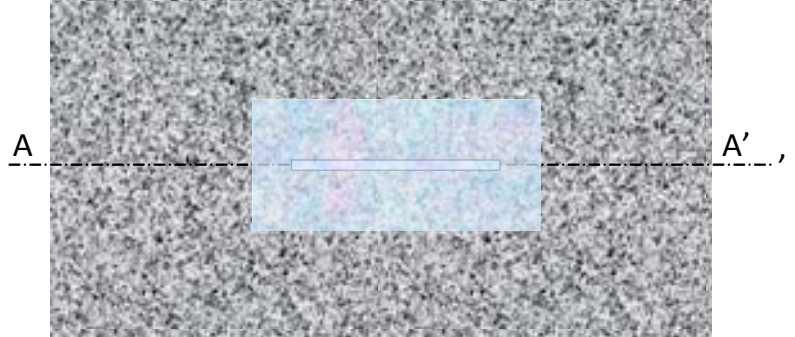
Spin coating develop 100 nm resist MET-2D



E-beam lithography resist opening



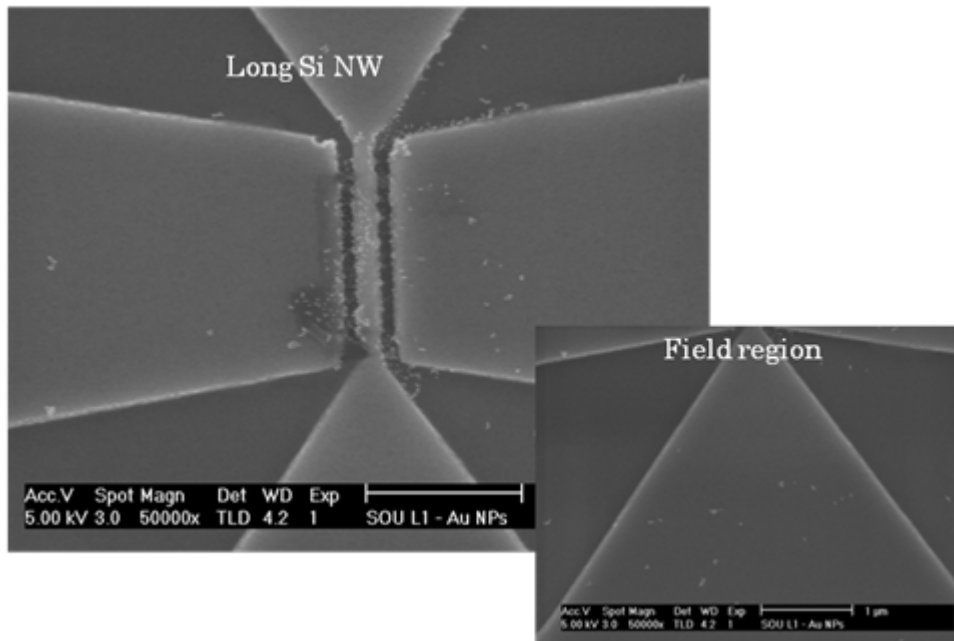
Selective resist removal



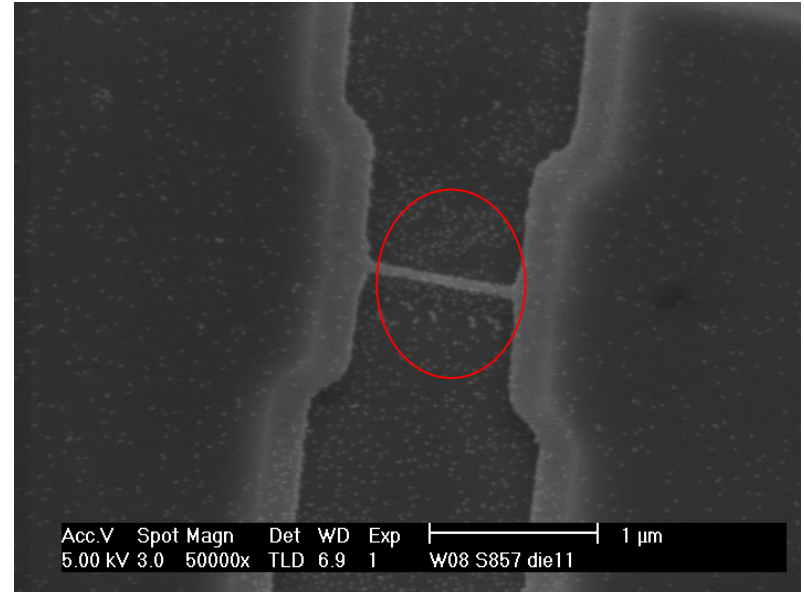
Short clean + NH₂-SAM deposition

Testing of selective functionalization with AuNPs

Nonsuspended SiNW



Suspended SiNW

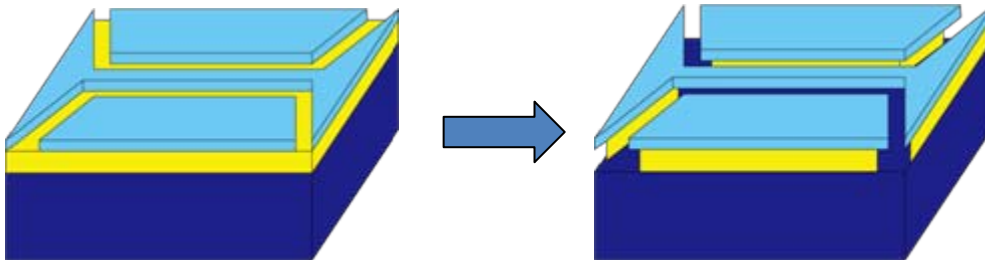


- ✓ Only SiNW region decorated by Au NPs (15 nm)
- ✓ Suspended Si NWs survived the spin coating of the polymer resist, ebeam lithography, resist removal in acetone and functionalization in toluene

Outline

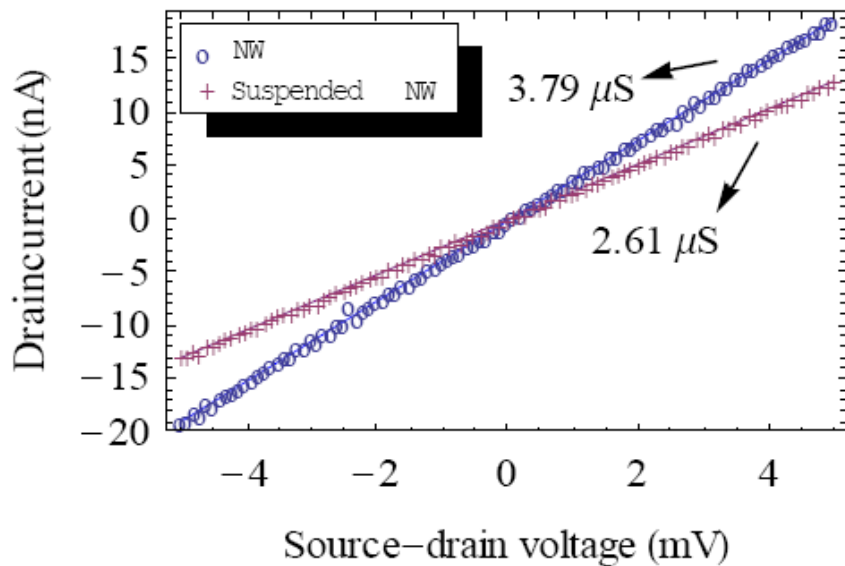
- Development of selective surface functionalization techniques for SiNWs
- SiNW electrical characteristics and the impact of suspension and surface functionalization
- Design and fabrication of in-plane resonant suspended gate FETs (IP-RSGFETs)
- Summary

Impact of SiNW suspension

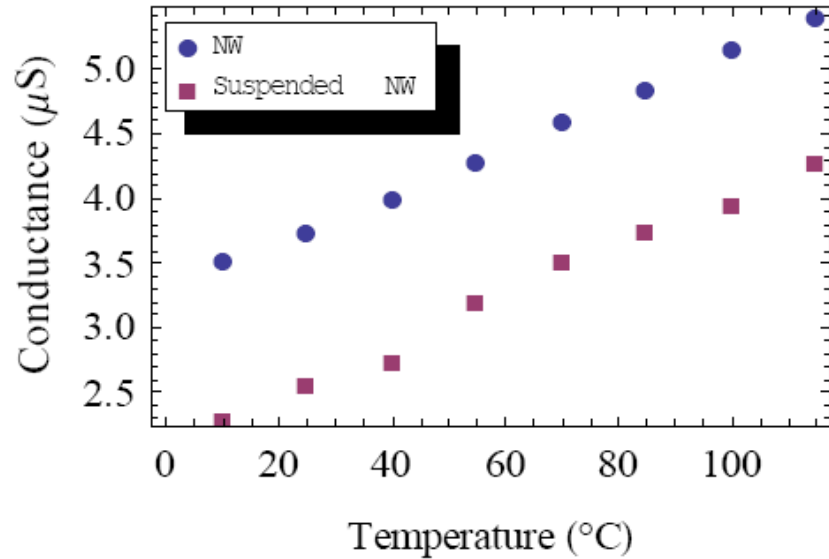


SOI $N_D = 2 \times 10^{19} \text{ cm}^{-3}$
SOI thickness $t_{\text{SOI}} = 53 \text{ nm}$
SiNW length $L = 0.5 - 2.0 \mu\text{m}$
SiNW width $W = 100 \text{ nm}$

I-V characteristics



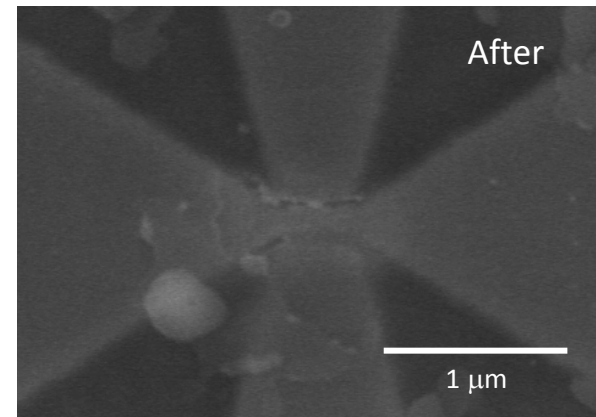
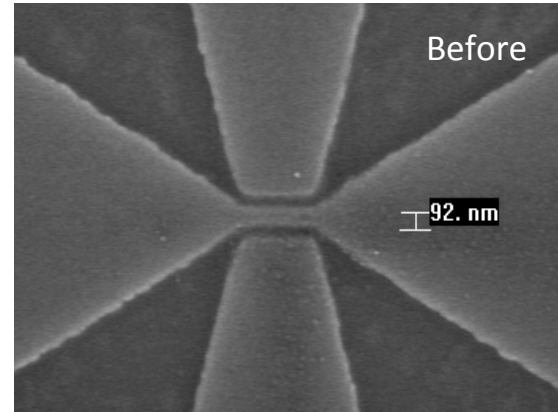
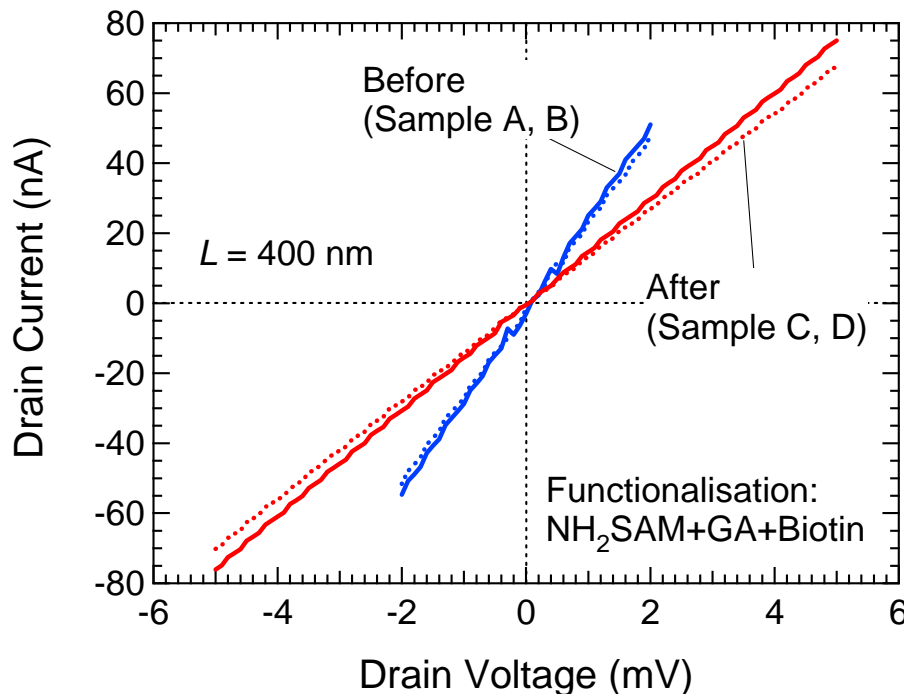
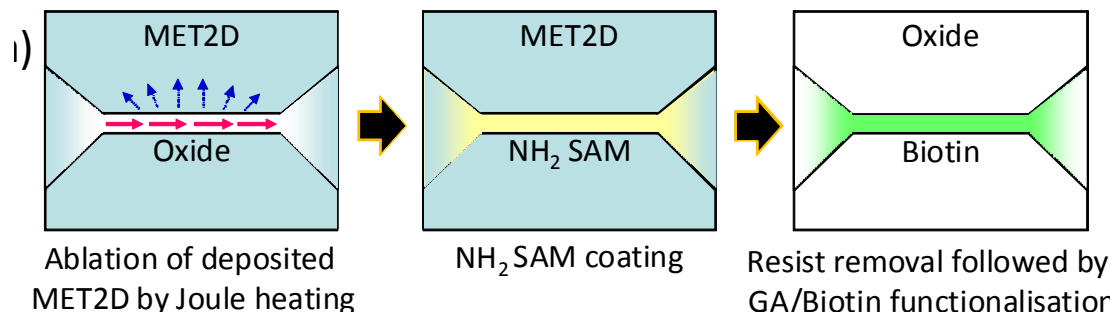
T dependence of G



- Conductance decreases after suspension
- Conductance increases with increasing temperature

Impact of bio-functionalisation

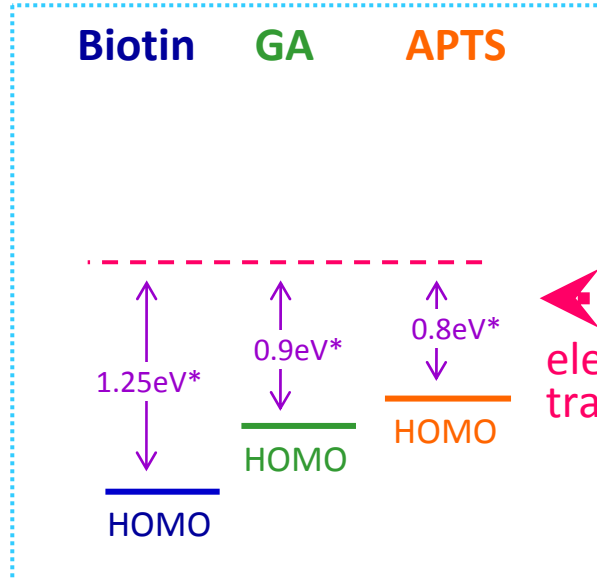
- Comparison between before and after bio-functionalisation



Conductance reduction after functionalisation

Possible charge transfer mechanism

SAM layers



Silicon nanowire

Oxide n⁺-SiNW

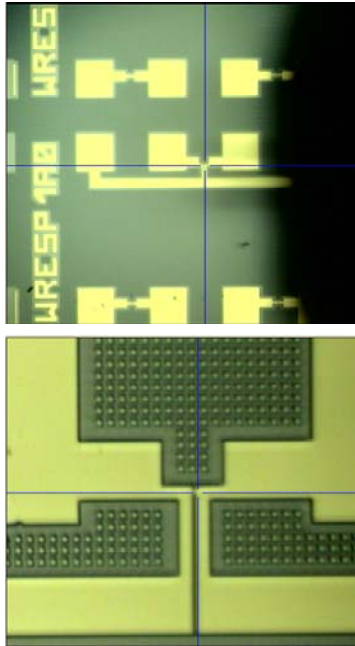
The figure shows two energy level diagrams. The left diagram is for $B = 0$, featuring a solid black parabolic curve representing the conduction band (E_c) and a dashed red parabolic curve representing the Fermi level (E_F). A vertical pink dashed line marks the point where the Fermi level intersects the conduction band. The right diagram shows the effect of increasing the external magnetic field B . The conduction band E_c remains relatively flat, while the Fermi level E_F shifts upwards and to the right, moving away from the conduction band edge.

Electron transfer
expected from SiNW to
surface molecular layers
results in conductance
reduction

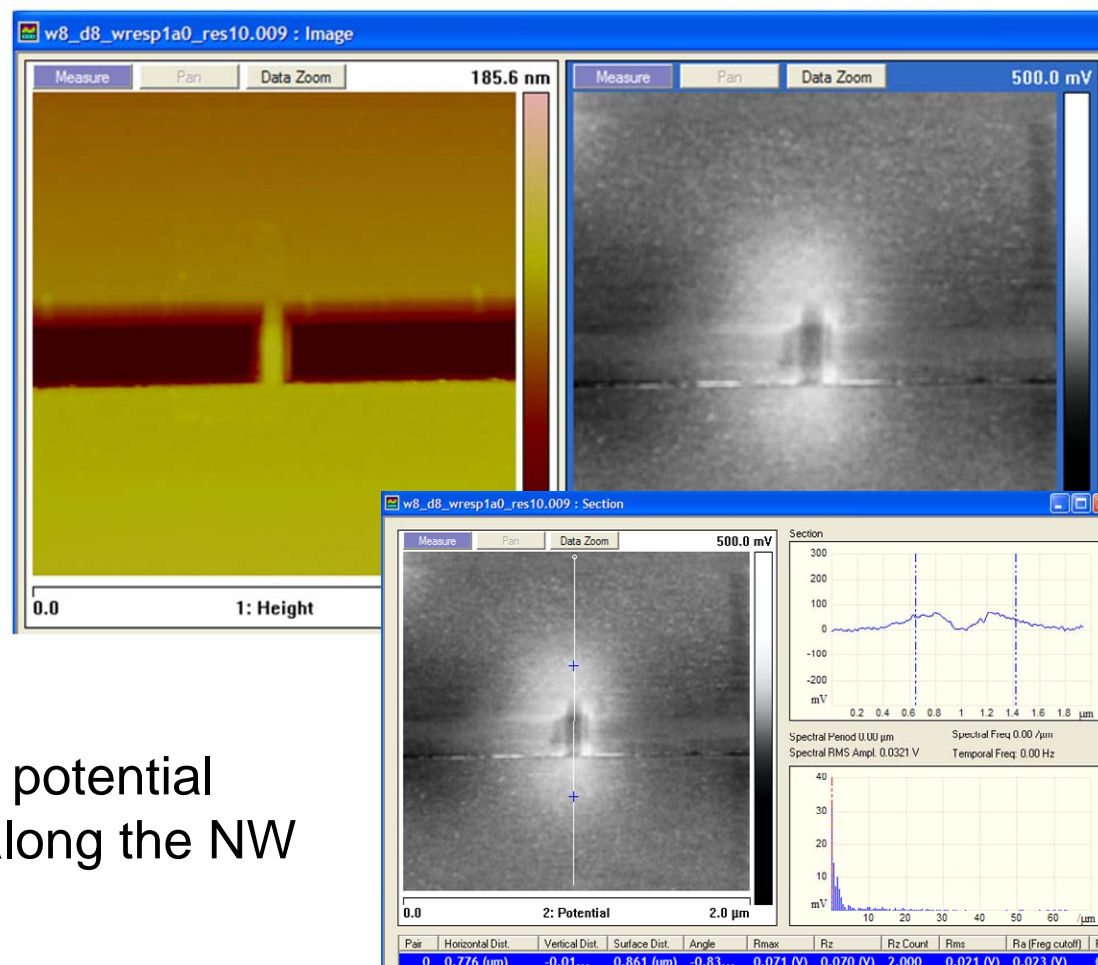
*All HOMO energies of organic molecules were estimated from the KFM results reported in D. M. Taylor et al., 'Characterization of chemisorbed monolayers by surface potential measurements', J. Phys. D: Appl. Phys. 24, 1443 (1991)

Surface potential distribution

Topography



Surface potential

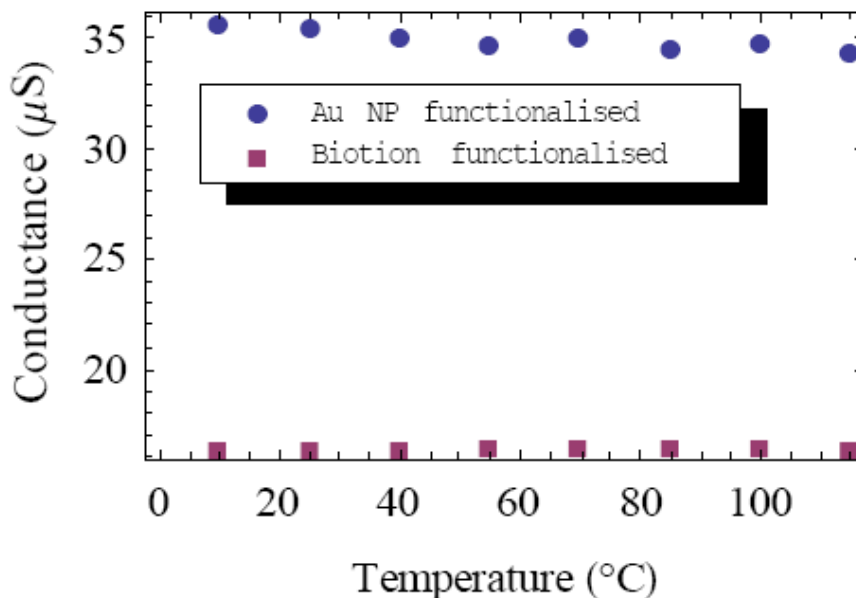


Surface potential profile along the NW

Surface potential shift in the cloudy rectangular area corresponds to the NH₂ SAM selective functionalization.

Temperature dependence of conductance

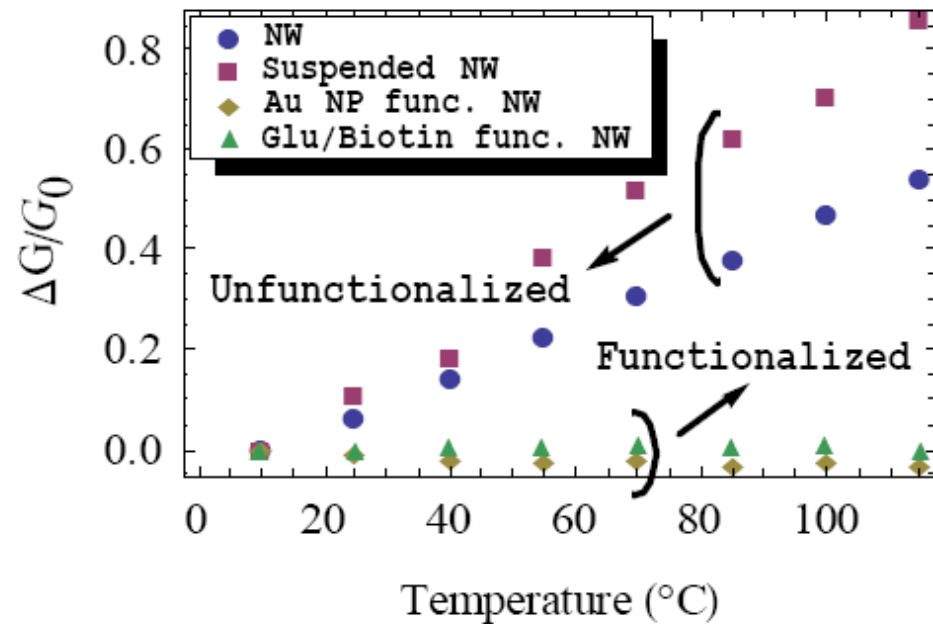
Conductance G vs T



Normalised conductance difference

$$\Delta G/G_0 = (G - G_0)/G_0 \text{ vs } T$$

G_0 : Conductance at $T = 10 ^{\circ}\text{C}$



After functionalisation

- $\Delta G/G_0$ is virtually temperature independent
- Regardless of the difference in functionalisation methods

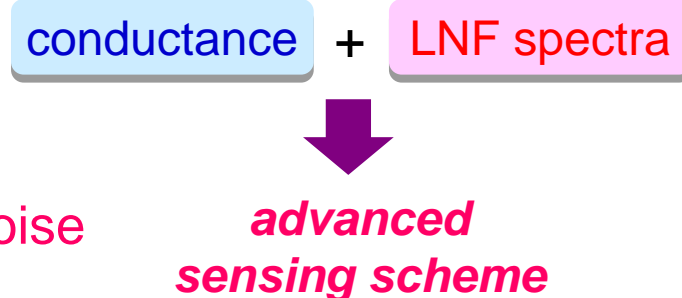
→ Advantageous for real sensing applications

SiNW LF noise spectra for advanced sensing scheme

Conduction noise in Si NW

Low frequency noise measurements

- ✓ To investigate the oxide/interface traps
- ✓ To explore a new sensing scheme using noise spectra beyond conductance detection



LF noise in Junctionless Transistor

Jang et al. Appl. Phys. Lett. **98**, 133502 (2011).

Hooge mobility fluctuation (HMF)

- Expected in bulk conduction

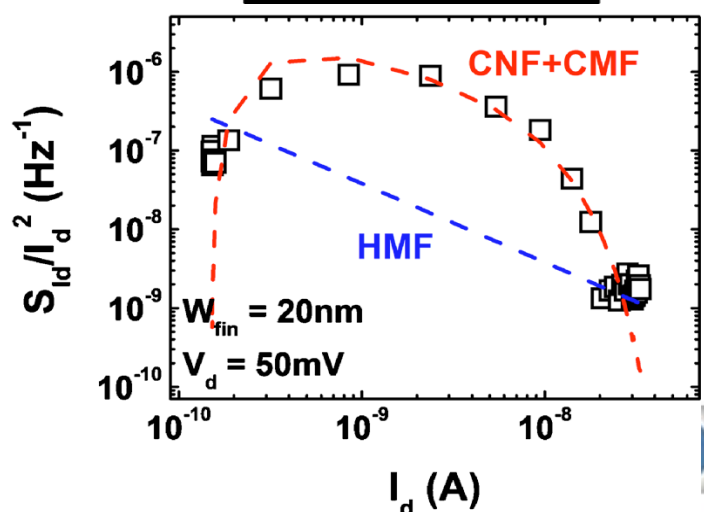
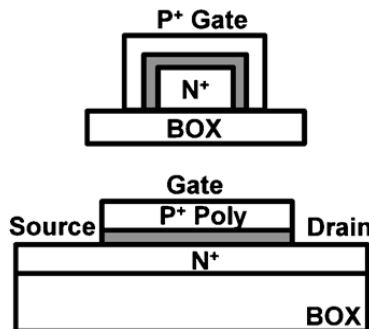
$$\frac{S_{Id}}{I_d^\beta} = \frac{\alpha_H}{N_c} \frac{1}{f^\gamma} = \frac{q\alpha_H \mu_{bulk} V_d}{f^\gamma I_d L^2}$$

Carrier number fluctuation correlated with carrier mobility fluctuation (CNF+CMF)

- Related to surface conduction

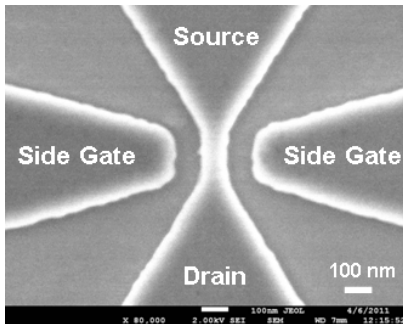
$$\frac{S_{Id}}{I_d^2} = S_{Vfb} \cdot \left(1 + \alpha_C \mu_{eff} C_{ox} \frac{I_d}{g_m}\right)^2 \cdot \left(\frac{g_m}{I_d}\right)^2$$

Results are rather consistent with CNF+CMF

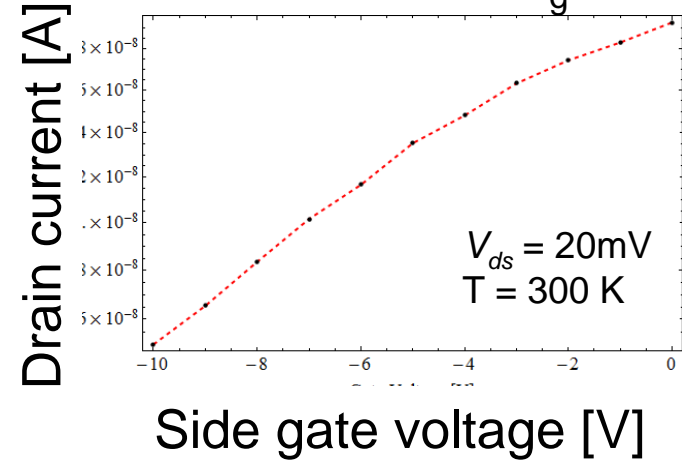


LF noise in non-suspended n-type SiNWs

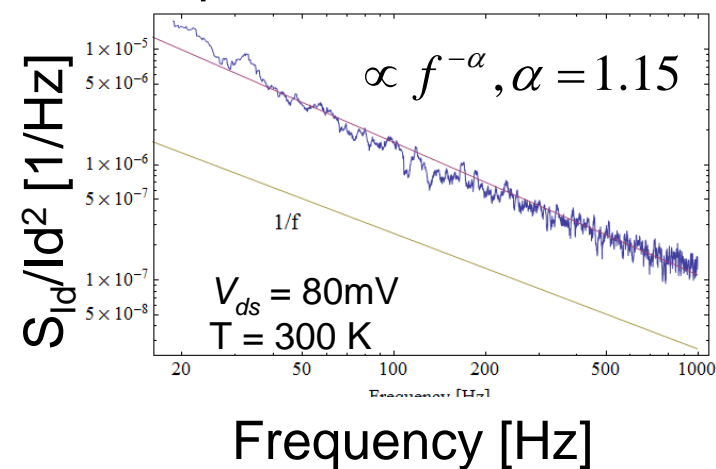
Device structure



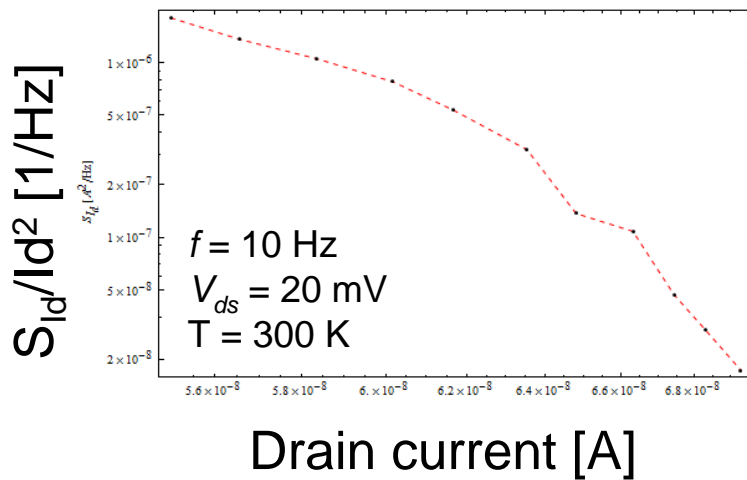
Conduction current vs V_g



Noise spectrum



Noise intensity vs I_d



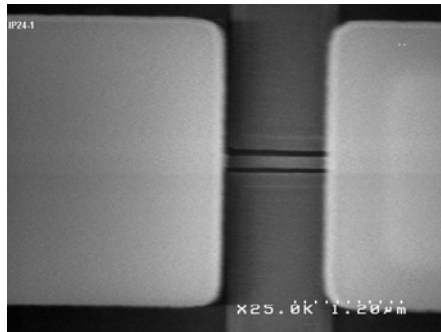
Noise intensity reduced with increasing drain current

- Indicating the result is related to mobility fluctuation but it is not clear whether this is with HMF or CNF+CMF
- Data should be taken by varying wider range of drain current

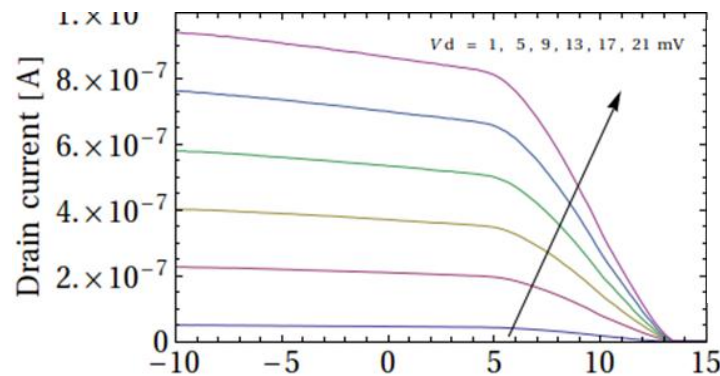
LF noise in suspended p-type SiNWs

(Preliminary)

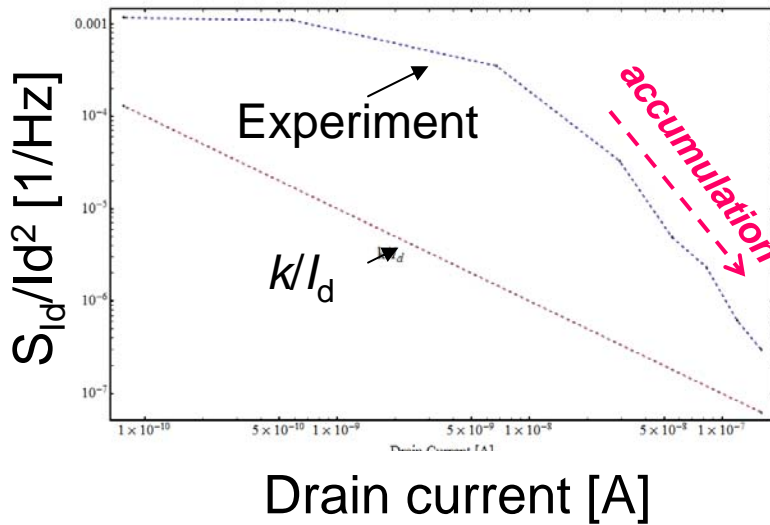
Device structure



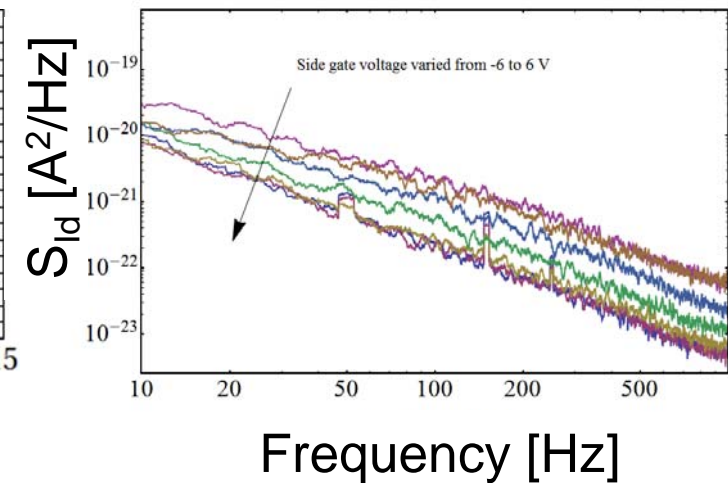
Conduction current vs V_g



Noise intensity vs I_d



Noise spectra



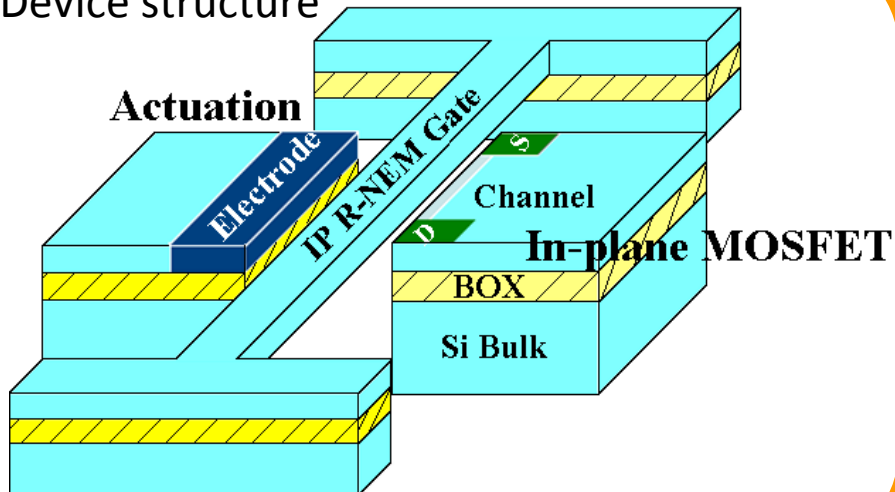
- I_d dependence of S_{Id}/I_d^2 is similar to the results of Jang et al's, i.e., (CNF+CMF)
- S_{Id}/I_d^2 in the **accumulation region** is governed by CNF at the surface and interface ⇒ may be used for advance sensing.

Outline

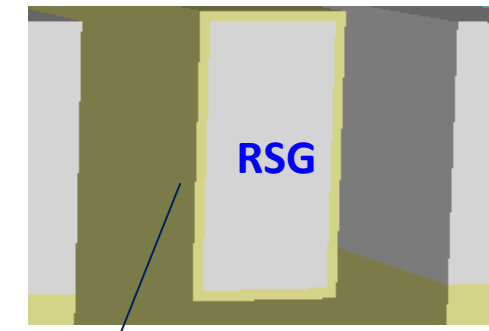
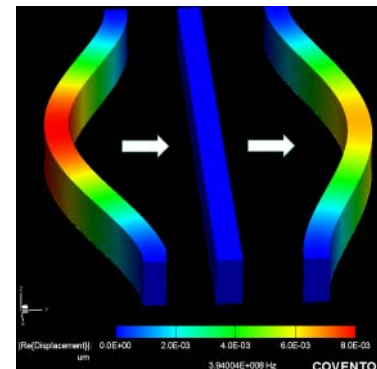
- Development of selective surface functionalization techniques for SiNWs
- SiNW electrical characteristics and the impact of suspension and surface functionalization
- Design and fabrication of in-plane resonant suspended gate FETs (IP-RSGFETs)
- Summary

Design of IP-RSGFETs for mass detection

Device structure

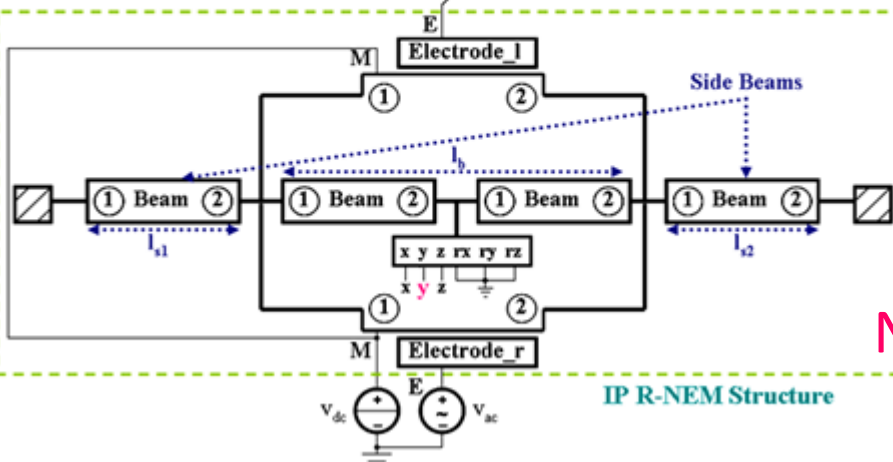
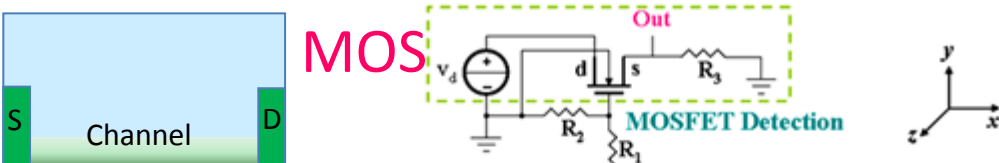


3D FEM analysis of RSG with surface layers using CoventorWare

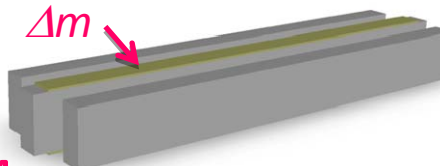


Surface functionalization & molecule adsorption /desorption

MOS



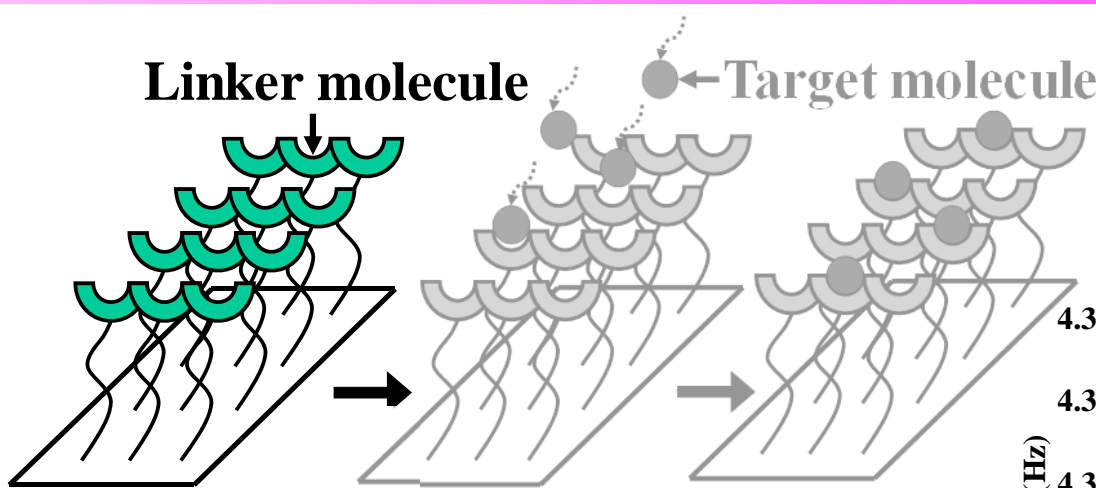
NEM



NEM-MOS hybrid circuit analysis using Architect

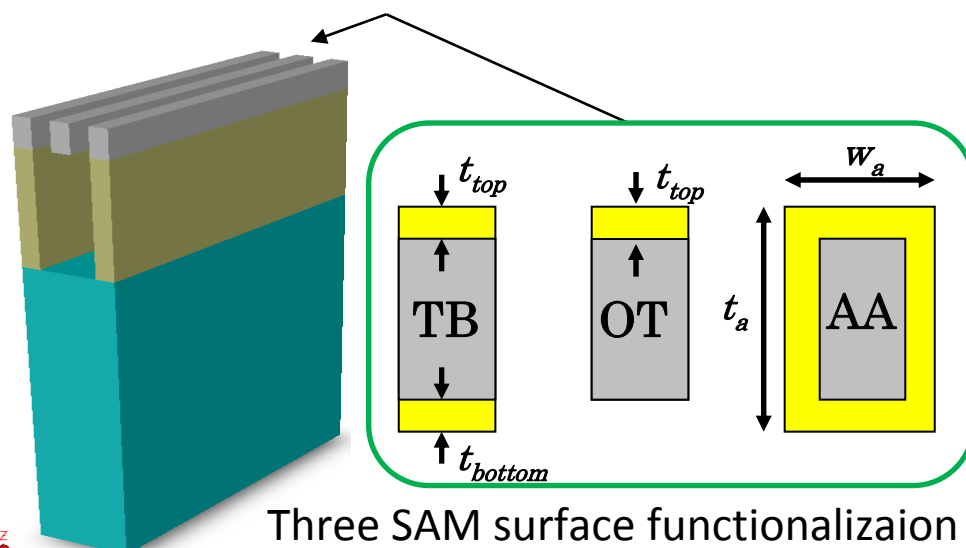


Surface layer modelling in 3D FEM analysis

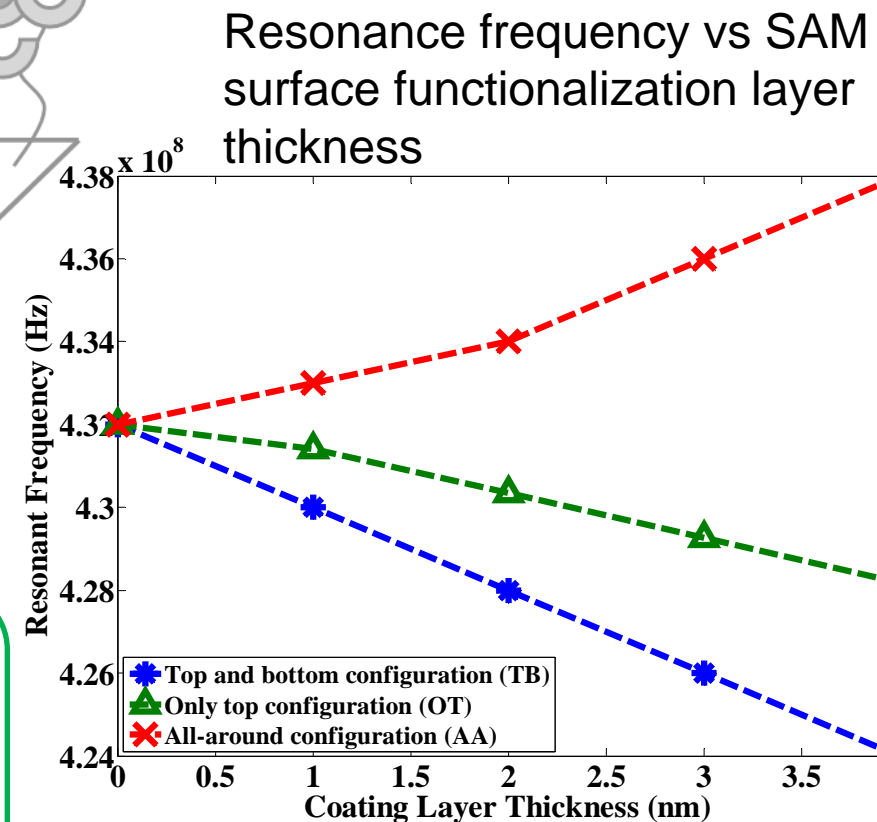


Functionalization

Molecule adsorption



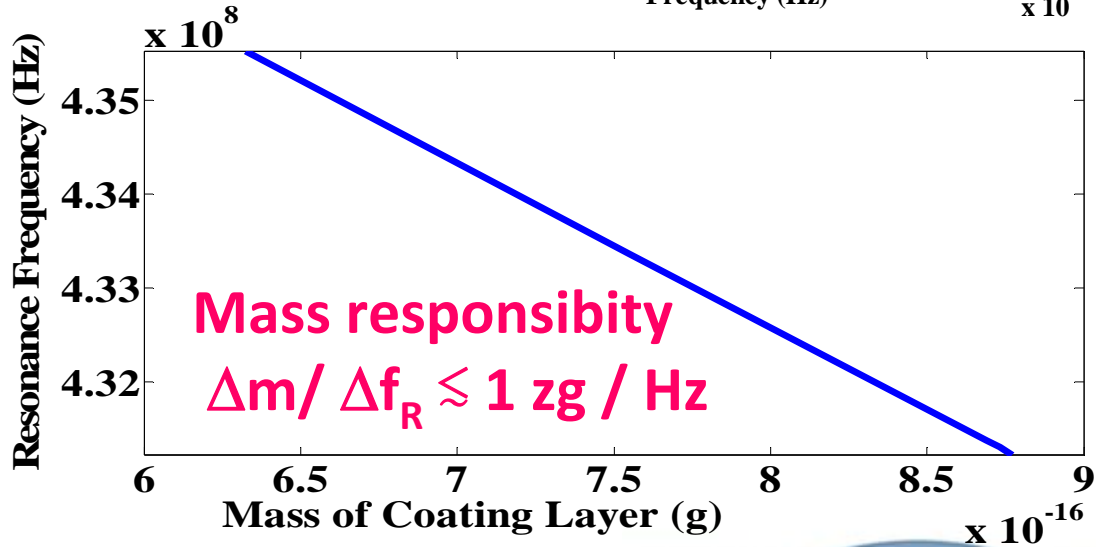
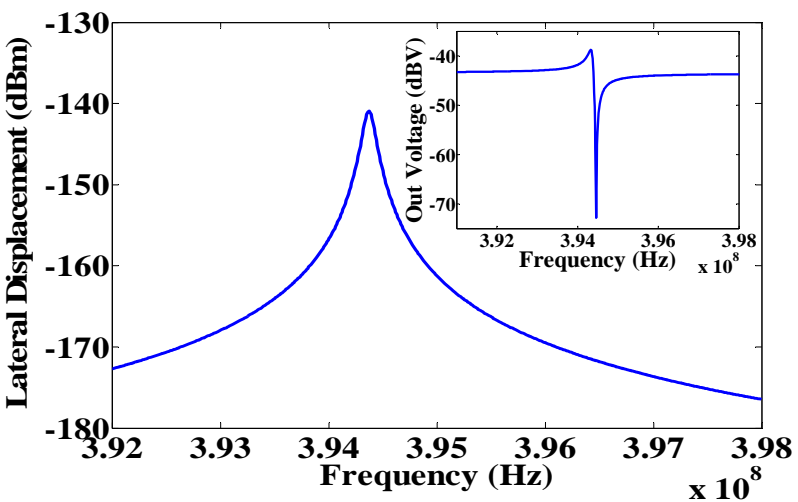
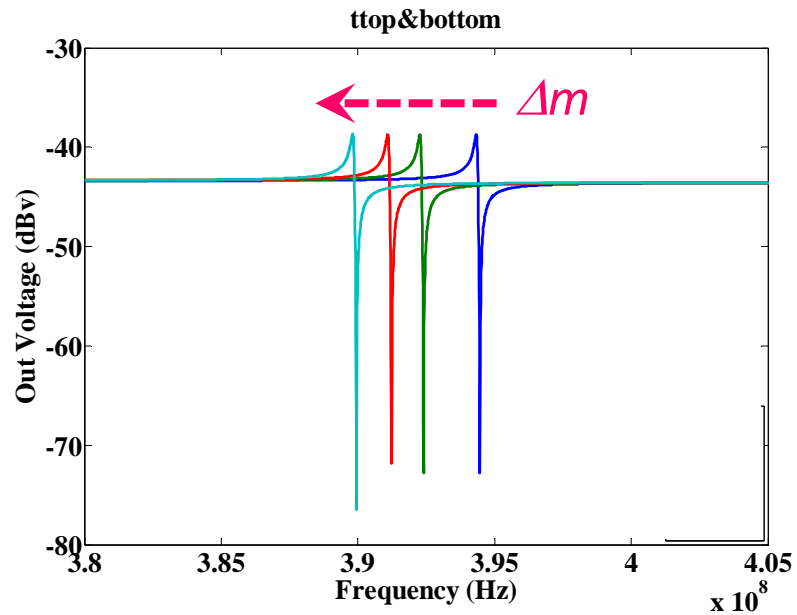
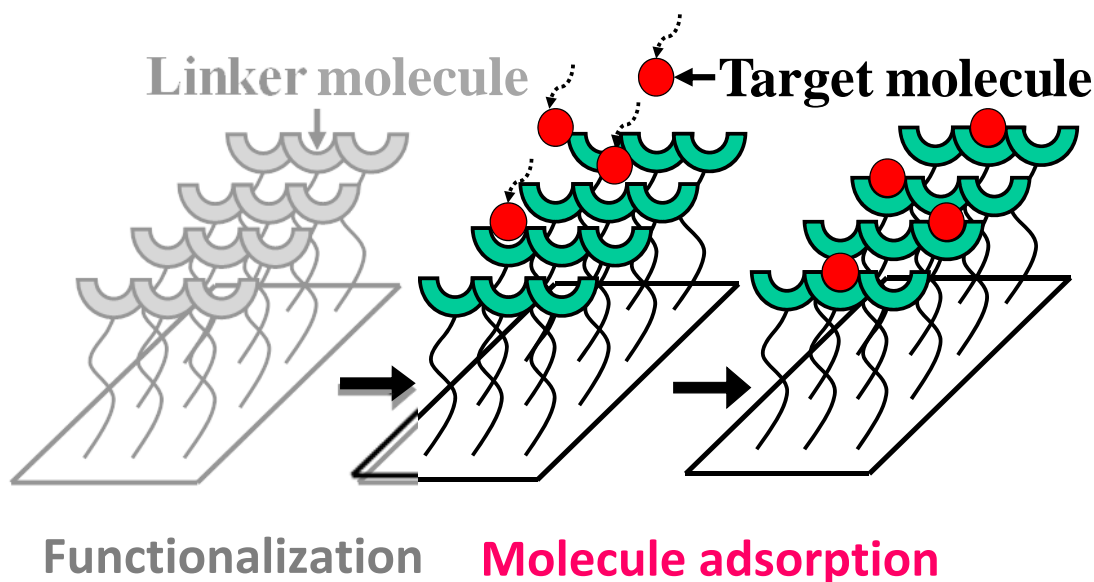
Three SAM surface functionalizaion layer configuration:
Top & Bottom (TB), Top only (OT), All around (AA)



RSG mass ↑ $f_R \downarrow$
RSG stiffness ↑ $f_R \uparrow$



Surface layer modelling in 3D FEM analysis



RSG Q-factor design

Quality factor analysis & advanced RSG design

Numerical modelling of Q-factor

$$\frac{1}{Q_{total}} = \frac{1}{Q_{air}} + \frac{1}{Q_{anchor}} + \frac{1}{Q_{structural}}$$

Q_{air} : dissipation in air

Q_{anchor} : through the anchors

$Q_{structural} = Q_{material} + Q_{thermoelastic}$

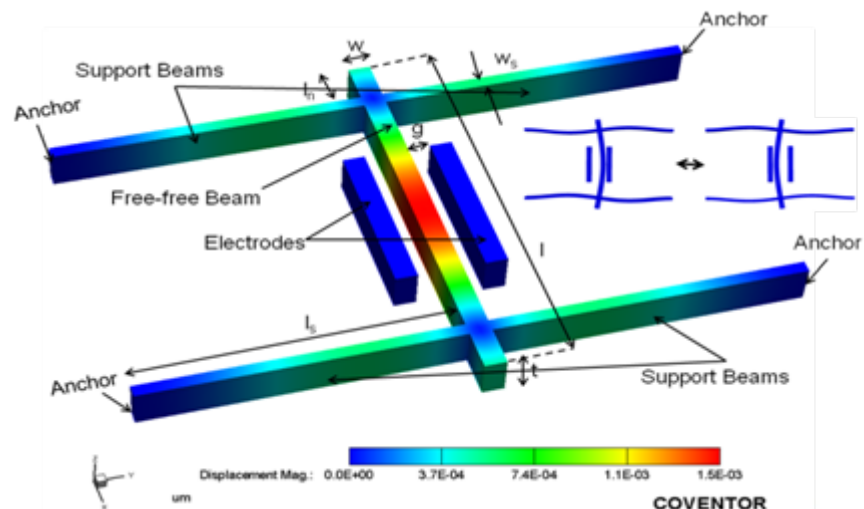
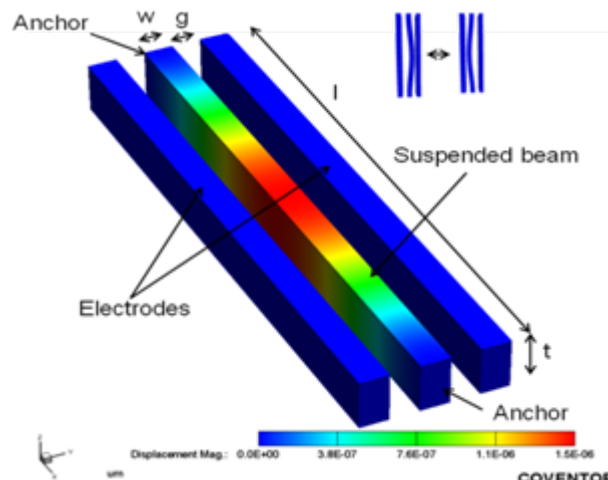
$Q_{material}$: material loss

$Q_{thermoelastic}$: thermoelastic damping

Clamped-clamped RSG



Free-free RSG



RSG Q-factor design

Clamped-clamped RSG

$$f_0 = 432.47 \text{ MHz}$$

$$b = 3.724 \times 10^{-12} (\text{N.s})/\text{m}$$

$$\text{Mass sensitivity} = 0.0544 \text{ zg/Hz}$$

$$Q_{\text{Air}} = 6245.97$$

$$Q_{\text{Thermoelastic}} = 680632.73$$

$$Q_{\text{Anchor}} = 3153.67$$

$$Q_{\text{Total}} = 2089.15$$

Free-free RSG

$$f_0 = 368.75 \text{ MHz}$$

$$b = 3.5632 \times 10^{-12} (\text{N.s})/\text{m}$$

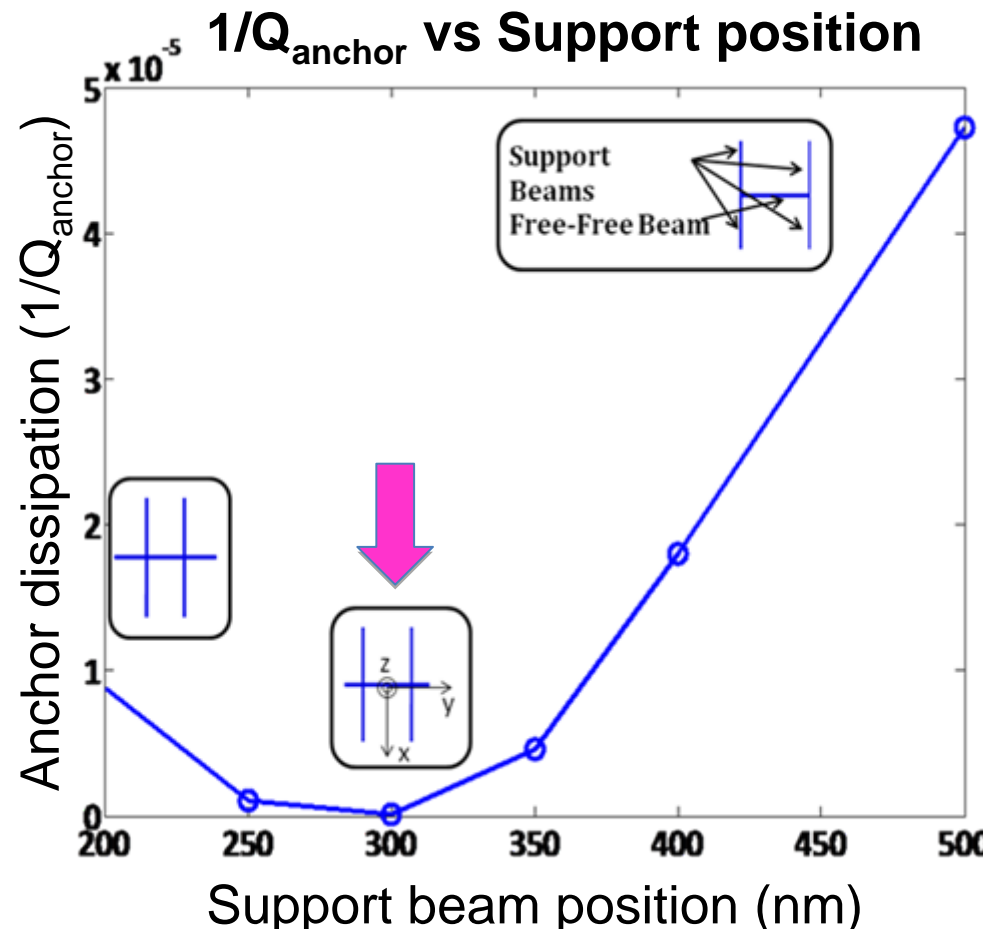
$$\text{Mass sensitivity} = 0.2363 \text{ zg/Hz}$$

$$Q_{\text{Air}} = 8348.71$$

$$Q_{\text{Thermoelastic}} = 1462838.84$$

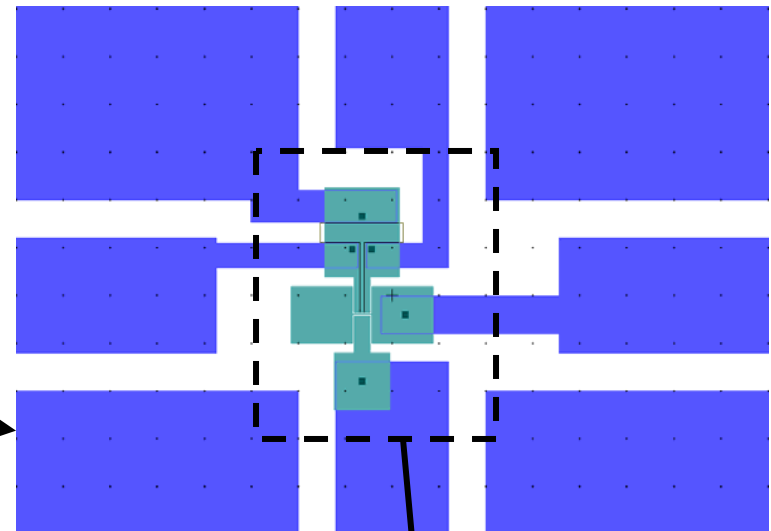
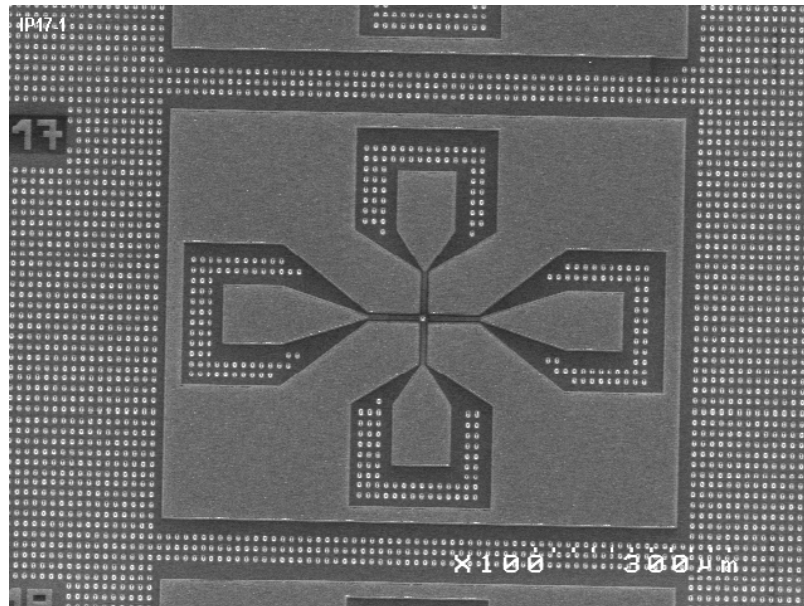
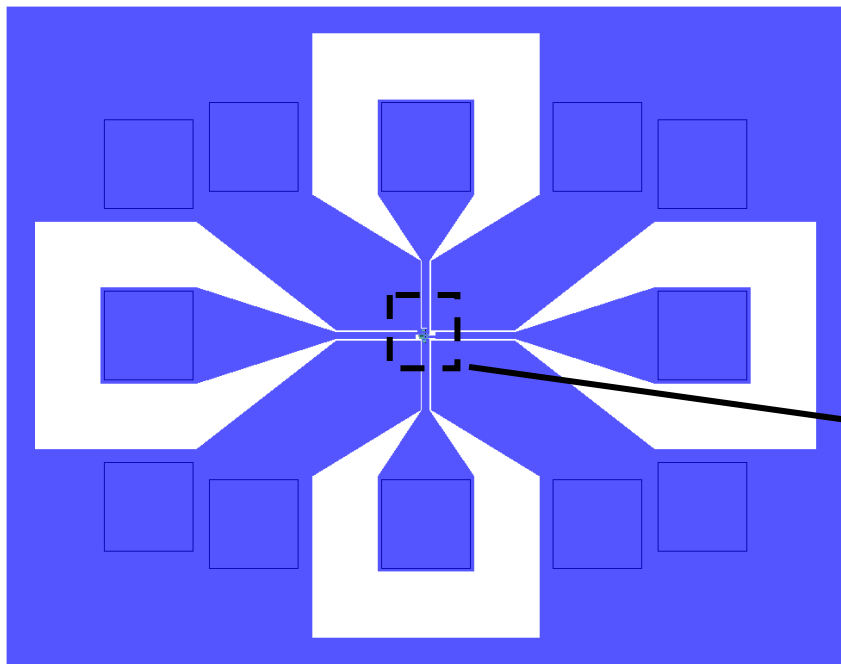
$$Q_{\text{Anchor}} = 10535972.28$$

$$Q_{\text{Total}} = 8294.79$$



Q-value can be optimized by adjusting the anchor positions of RSG

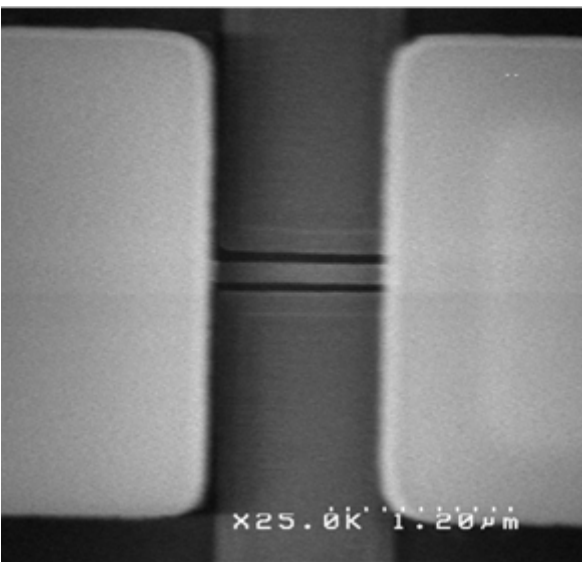
IR-RSGFET design layout



Suspended gate (SG)
Source Drain

- L_{SG} : 1000 - 2000 nm
- W_{SG} : 45 – 135 nm
- SG – MOS air gap: 80 – 200nm

Preliminary IR-RSGFET characteristics (DC)



Suspended gate:

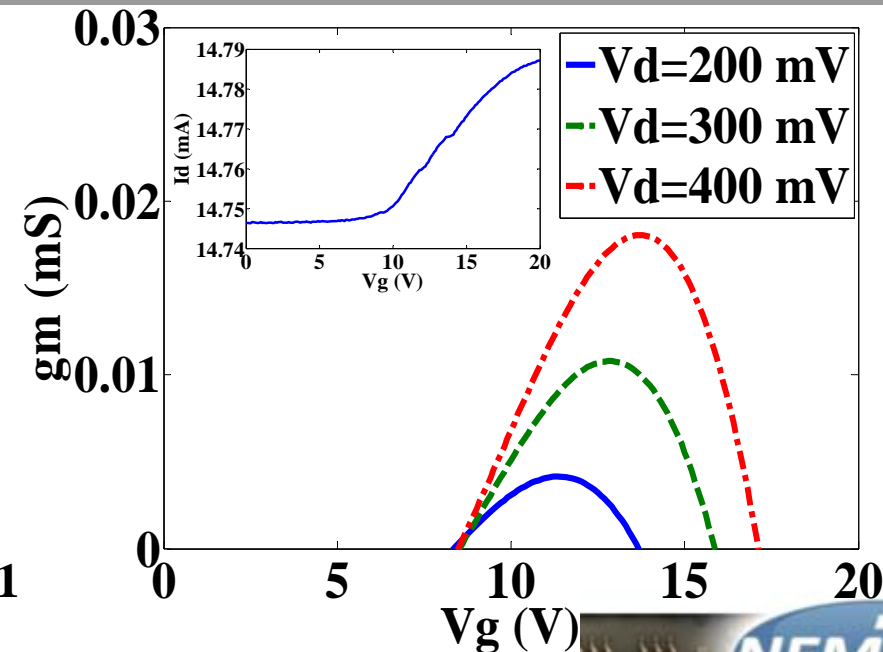
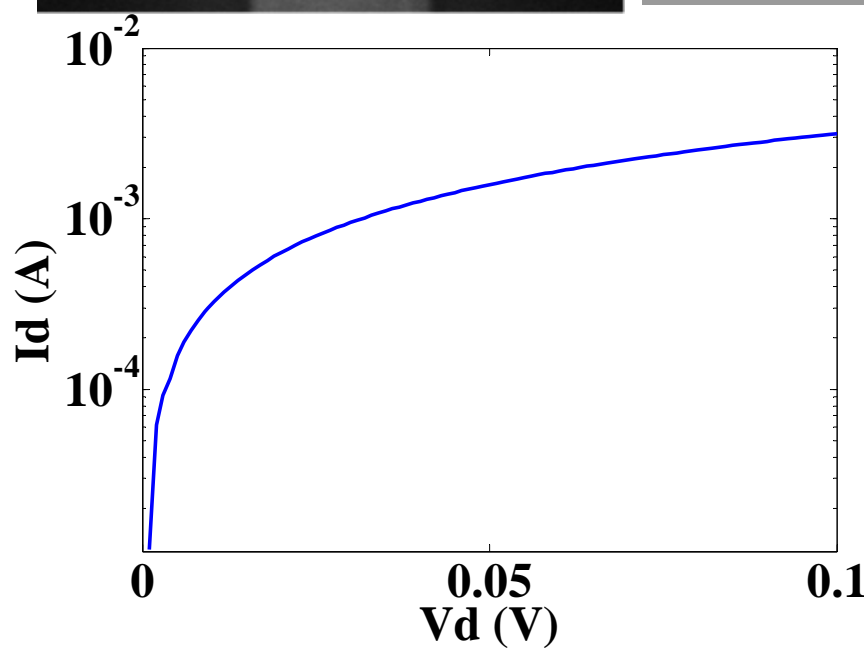
Width=135 nm, Length=2000 nm, Thickness=40 nm
SG – MOS air gap = 80nm

In-plane MOSFET:

Channel length=1250 nm, Drain/Source length=295 nm

Doping:

Drain/Source /Suspended gate = (N^+) 4×10^{19} at.cm $^{-3}$,
Channel=(P) 1×10^{16} at.cm $^{-3}$



Optimal $V_d = 400$ mV & $V_g = 14$ V will be used for the subsequent RF measurement

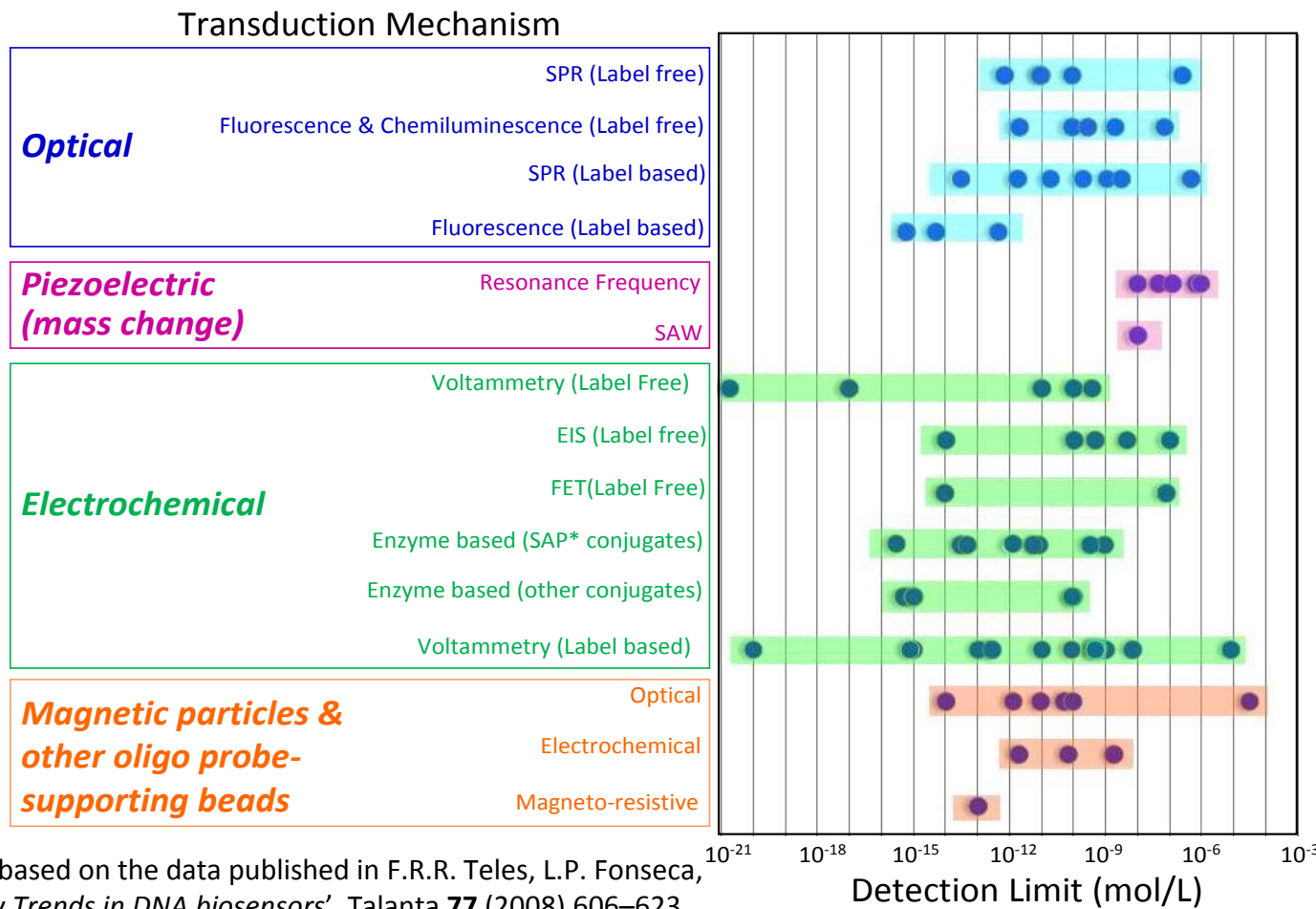
Summary

- Selective surface biofunctionalization techniques were developed successfully for suspended SiNWs: Joule heating method & ebeam lithography method.
- Detectable change in the conductance was observed with SiNW suspension and surface functionalization. Preliminary LFN spectra are studied for advanced sensing beyond conductance detection.
- IP-RSGFETs with zeptogram/Hz level mass responsivity were designed using new hybrid NEM-MOS simulation. Preliminary DC characteristics were measured for fabricated IP-RSGFETs.



Conductance or Mass?

DNA detection limit based on various transduction mechanisms



Drawn based on the data published in F.R.R. Teles, L.P. Fonseca,
'Review Trends in DNA biosensors', Talanta **77** (2008) 606–623.